Ultramicroscopy 169 (2016) 107–121

Contents lists available at ScienceDirect

Ultramicroscopy

journal homepage: www.elsevier.com/locate/ultramic

# Practical aspects of diffractive imaging using an atomic-scale coherent electron probe

Z. Chen [a,*], M. Weyland [b,c], P. Ercius [d], J. Ciston [d], C. Zheng [a,e], M.S. Fuhrer [a], A.J. D'Alfonso [f], L.J. Allen [f], S.D. Findlay [a]

[a] School of Physics and Astronomy, Monash University, Clayton, Victoria 3800, Australia
[b] Monash Centre for Electron Microscopy, Monash University, Clayton, Victoria 3800, Australia
[c] Department of Materials Science and Engineering, Monash University, Clayton, Victoria 3800, Australia
[d] National Center for Electron Microscopy, Molecular Foundry, Lawrence Berkeley National Laboratory, Berkeley, CA 94720, USA
[e] Department of Civil Engineering, Monash University, Clayton, Victoria 3800, Australia
[f] School of Physics, University of Melbourne, Parkville, Victoria 3010, Australia

ARTICLE INFO

*Article history:*
Received 14 April 2016
Received in revised form
16 June 2016
Accepted 23 June 2016
Available online 25 June 2016

*Keywords:*
Diffractive imaging
Convergent beam electron diffraction
Differential phase contrast
Phase reconstruction

ABSTRACT

Four-dimensional scanning transmission electron microscopy (4D-STEM) is a technique where a full two-dimensional convergent beam electron diffraction (CBED) pattern is acquired at every STEM pixel scanned. Capturing the full diffraction pattern provides a rich dataset that potentially contains more information about the specimen than is contained in conventional imaging modes using conventional integrating detectors. Using 4D datasets in STEM from two specimens, monolayer $MoS_2$ and bulk $SrTiO_3$, we demonstrate multiple STEM imaging modes on a quantitative absolute intensity scale, including phase reconstruction of the transmission function via differential phase contrast imaging. Practical issues about sampling (i.e. number of detector pixels), signal-to-noise enhancement and data reduction of large 4D-STEM datasets are emphasized.



## 1. Introduction

Convergent beam electron diffraction (CBED) patterns acquired using an atomic size coherent probe in scanning transmission electron microscopy (STEM) contain rich structural information. However, traditional STEM experiments such as bright field (BF) or annular dark field (ADF) use monolithic detectors that integrate over many points in the diffraction plane to allow fast acquisition and high signal-to-noise ratio (SNR). Though position-resolved electron diffraction has a long history [1–3], the slow readout speed of the conventional CCD camera, limited data transfer speed and limited storage space have restricted acquisition to a small number of frames, making atomic resolution diffractive imaging extremely challenging [4]. Recent developments in fast-readout pixel detectors and powerful computers significantly improve the speed of data acquisition and transfer, and make possible the acquisition of two-dimensional CBED patterns with two dimensional probe scanning positions – a four dimensional (4D) dataset – at atomic resolution [5–7]. Such 4D datasets have been shown to allow synthesizing multiple imaging modes [4,8], differential phase contrast imaging [6] and ptychographic phase reconstruction [7,9]. However, the full potential of 4D datasets for quantitative analysis has yet to be established. The huge size of the 4D datasets also makes data storage, transfer and analysis challenging. Therefore, approaches to reducing the data size while conserving the information of interest are highly desirable.

In this paper, we demonstrate quantitative imaging on an absolute intensity scale for both coherent and incoherent STEM image modes, including differential phase contrast imaging and quantitative phase reconstruction. Practical experimental considerations, such as detector extent and sampling (i.e. number of detector pixels), SNR and information content are also discussed with a view to providing guidelines for future experiments.

## 2. Experimental methods and data processing

The experiments were carried out on the TEAM I electron microscope at the National Center for Electron Microscopy (NCEM) facility of the Molecular Foundry in Berkeley, California, operating at 300 kV. Using an atomic size probe, CBED patterns were acquired at each probe position using a Gatan K2-IS direct detection camera operated in a linear mode at 400 frames per second. Each CBED pattern has $1920 \times 1792$ pixels and patterns with up to

* Corresponding author.
*E-mail address:* zhen.chen@monash.edu (Z. Chen).

http://dx.doi.org/10.1016/j.ultramic.2016.06.009
0304-3991/

256 × 256 scanning probe positions were acquired, giving raw datasets of several hundred gigabytes (GBs). The data were first distilled into *.dm4 format files from the raw binary data using the Gatan in situ imaging plugin. The *.dm4 files were then read into MATLAB using an efficient and fast script [10]. The default MATLAB file (*.mat), an HDF5-based format storing the data in compressed chunks, was used in the following data analysis employing custom MATLAB codes. To treat huge datasets – several hundred GBs in size, much larger than the random-access memory installed in most computers – the datasets were loaded into the memory sequentially, facilitated by the fast read and write speed of the solid state disks (SSDs) (in our case quad striped PCIe bus SSDs). Reading and writing in data stacks instead of single frames or pixels was used to reduce the reading and writing times and accelerate the data analysis.

Two materials were chosen in this study, monolayer $MoS_2$ and bulk $SrTiO_3$. Monolayer $MoS_2$ is a weakly scattering material, making it suitable for differential phase contrast imaging since the phase-object approximation is expected to be satisfied. $SrTiO_3$ is a well-known perovskite structure with both light and heavy atomic columns and is widely used for testing new imaging techniques, making it a suitable test case for exploring quantitative imaging from a variety of imaging modes. The experiments on $MoS_2$ used a convergence semi-angle of $\alpha = 17.1$ mrad which, for an ideally coherent probe, corresponds to a diffraction limited probe size of 1.1 Å, and a beam current of about 48 pA, as read from the viewing screen which was calibrated using the drift tube of a Gatan spectrometer. The experiments on $SrTiO_3$ used $\alpha = 21.3$ mrad (probe size 0.9 Å) and a beam current of about 65 pA, with data taken from multiple areas of differing thickness. A high-angle annular dark-field (HAADF) image was acquired simultaneously with the 4D datasets. HAADF images before and after the 4D dataset acquisition were also taken to monitor the beam damage: only those datasets with modest change between before and after HAADF images were chosen for the data analysis.

The thicknesses of the different regions of $SrTiO_3$ examined were determined by the $L^2$-norm method [11,12] from the position averaged CBED (PACBED) pattern obtained by averaging the 4D dataset. A two-dimensional (2D) Gaussian function was assumed to account for the spatial incoherence, taken to include both the effective source size and additional broadening introduced by the repeat unit averaging procedure (discussed below) used to correct specimen drift and improve SNR. The Gaussian width was determined by comparing the averaged experimental HAADF images acquired simultaneously with the 4D dataset acquisition with HAADF images simulated using the quantum excitation of phonons method implemented in the software $\mu$STEM [13,14]. The half-width half-maximum (HWHM) thus determined is approximately 0.45 Å for $MoS_2$ and 0.50 Å for $SrTiO_3$. The incident beam intensity for image normalization was measured by taking one aperture image in vacuum for each experimental condition using the same camera. In the case of $SrTiO_3$, there was some evidence of variation of the beam current during experiments, which was attributed to monochromator settings or gun alignment change. To compensate for this, a single multiplicative factor of 0.86 was applied to all $SrTiO_3$ datasets prior to quantitative image comparison with the simulations. This factor is consistent with the difference between the total integrated intensity of the whole PACBED pattern of each dataset (scattering angle up to $4\alpha$ for $SrTiO_3$) and the total intensity from the aperture image in vacuum, to within the uncertainty introduced by the relatively large variations of the dark current reference and weak SNR at high scattering angles in the CBED patterns. (Note that simulations show the percentage of electron intensity scattered outside the scattering angle of $4\alpha$ is less than 1% for even the thicker specimen region considered.).

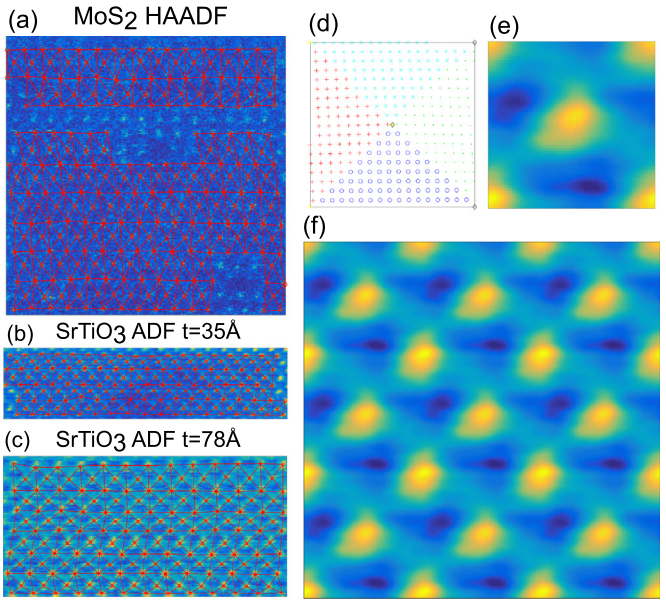


**Fig. 1.** Raw images used for scanning drift correction: (a) HAADF image of $MoS_2$ acquired simultaneously with the 4D dataset; (b) and (c) synthesized ADF images for a 35 Å and 78 Å thick region of $SrTiO_3$ respectively. The circles indicate the column positions and the lines show the triangular patches. (d) The coordinates of the image pixels after the affine transformation of a single unit-cell area patch in (c). (e) Averaged unit-cell image for the 78 Å thick region of $SrTiO_3$. (f) A 3 × 3 unit-cell tiling of the image in (e) for visualization purposes. (For interpretation of the references to color in this figure caption, the reader is referred to the web version of this paper.).

Whereas conventional HAADF STEM imaging is carried out with a dwell time on the order of tens of microseconds, acquisition of the full diffraction patterns on the K2-IS camera necessitated a dwell time of 2.5 ms per pixel, a much slower scan. Consequently, specimen drift becomes a substantial problem. In addition, the fine pixel size in the CBED patterns means a poor SNR at each individual pixel. Using the simultaneously acquired HAADF image (or a suitably robust synthesized image) as a structural reference, shown in Fig. 1(a)–(c), the known structure of $MoS_2$ and $SrTiO_3$ was used to correct scanning drift via a local geometric image transformation method [15]. The main steps in this method are as follows. A normalized cross-correlation method is used to determine the coordinates of the atomic column positions. Next, the reference image is partitioned into a disjoint triangular mesh with these column positions as vertices: nearest neighbor Sr–Sr–Ti triangles in $SrTiO_3$ and Mo–Mo–Mo triangles in $MoS_2$. The red lines overlaid onto the images shown in Fig. 1(a)–(c) illustrate the triangular patches. The evidently damaged areas in the $MoS_2$ specimen were not included during the averaging procedure. For each triangle, an affine transformation matrix is then defined that maps the three vertices from the reference image to their expected configuration based on the known model structure. An example of the coordinates of the image pixels after the affine transformation of one unit-cell area from Fig. 1(c) is shown in Fig. 1(d). The transformation matrix thus set up is then applied to map each experimental point within each triangular template to a fractional coordinate $\mathbf{R}_j$ within the unit cell. Due to specimen drift and sampling, the set of positions $\{\mathbf{R}_j\}$ thus defined is not on a regular mesh and so cannot readily be visualized. However, based on the periodicity of the crystal structure, the measured STEM image intensities at the points $\mathbf{R}_j$ can be related to the Fourier coefficients of the STEM image $I_{\mathbf{G}}$ via

$$I(\mathbf{R}_j) = \sum_{\mathbf{G}} I_{\mathbf{G}} e^{2\pi i \mathbf{R}_j \cdot \mathbf{G}}. \quad (1)$$